

## Supplementary Information

### **Insertion of a methylene group into the backbone of an antisense oligonucleotide reveals importance of deoxyribose recognition by RNase H**

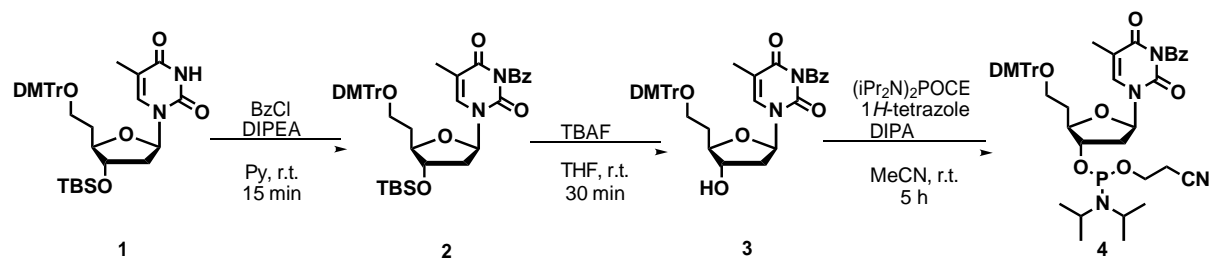
Yoshiaki Masaki<sup>1,2\*</sup>, Ayano Tabira<sup>1</sup>, Shihori Hattori<sup>1</sup>, Shunsuke Wakatsuki<sup>1</sup>, Kohji Seio<sup>1</sup>

<sup>1</sup> Department of Life Science and Technology, Tokyo Institute of Technology, 4259-J2-16 Nagatsuta, Midori, Yokohama, Kanagawa, 226-8501, JAPAN. <sup>2</sup> PRESTO, JST 4-1-8 Honcho, Kawaguchi, Saitama, 332-0012, JAPAN.

\* To whom correspondence should be addressed. Tel: +81-45-924-5750; E-mail: ymasaki@bio.titech.ac.jp

## CONTENT

Scheme S1. Synthesis of <i>N</i> -benzoyl protected 5'-HMT phosphoramidite derivative. ....	4
General chemistry .....	5
Synthesis of compound 2.....	5
Synthesis of compound 4.....	6
Preparation of oligonucleotides .....	7
UV melting experiments.....	8
RNase H cleavage patterns .....	8
Figure S1. MALDI-TOF-MS chart of HTT-targeting antisense oligonucleotides. ....	10
Figure S2. Melting curves of each oligonucleotide with RNAs. ....	11
Figure S3. E. Coli RNase H (2RN2) and human RNase H1 catalytic domain (2QK9).....	20
Table S1. Positional relative kinetic constants ( $k_{rel_i}$ ) of 5'-HMT modification. ....	21
Table S2. Positional relative kinetic constants ( $k_{rel_i}$ ) of 3'-HMT modification. ....	21
Derivation of equations used in this study.....	22
Figure S4. Heatmap of observed $pm_i(mm)$ and calculated $pm_i(mm)$ .....	23
Figure S5. MALDI-TOF-MS chart of Cxcl12-targeting antisense oligonucleotides.....	24
Figure S6. Reverse phase-HPLC chart of purified antisense oligonucleotides used in this study. ....	25
<sup>1</sup> H-NMR of compound 2 .....	26
<sup>13</sup> C-NMR chart of compound 2 .....	26
<sup>1</sup> H-NMR of compound 4 .....	27
<sup>13</sup> C-NMR chart of compound 4 .....	27
<sup>31</sup> P-NMR chart of compound 4 .....	28

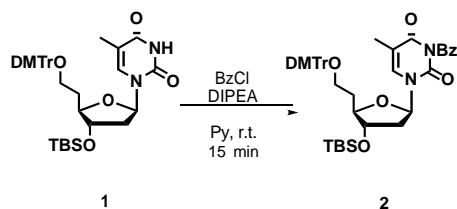


**Scheme S1.** Synthesis of *N*-benzoyl protected 5'-HMT phosphoramidite derivative.

## General chemistry

All chemical reagents and dry solvent were purchased from Tokyo Chemical Industry, FUJIFILM-Wako Pure Chemical Corporation, Kanto Chemical Co., Inc., Nakalai Tesque, and Sigma-Aldrich, and used as received. Phosphoramidite monomers of locked nucleic acid (LNA) were purchased from Hongene Biotech Corporation. Phosphoramidite monomer of 5-methyl-2'-deoxycytosine was purchased from LINK technology. The other phosphoramidite monomers were purchased from Glen Research. Ribonuclease H was purchased from TaKaRaBio, Inc. The Ultrapure™ DNase/Rnase-Free Distilled water was purchased from ThermoFisher Scientific.  $^1\text{H}$ ,  $^{13}\text{C}$ , and  $^{31}\text{P}$  nuclear magnetic resonance (NMR) spectra were recorded at 400, 101, and 162 MHz for  $^1\text{H}$ ,  $^{13}\text{C}$ , and  $^{31}\text{P}$  NMR, respectively. The chemical shifts were measured from residual non-deuterated solvent of  $\text{CDCl}_3$  (7.26 ppm) and  $\text{DMSO-}d_6$  (2.50 ppm) for  $^1\text{H}$  NMR spectra and solvent signal of  $\text{CDCl}_3$  (77.16 ppm) and  $\text{DMSO-}d_6$  (39.52 ppm) for  $^{13}\text{C}$  NMR spectra and 85% phosphoric acid (0.00 ppm) for  $^{31}\text{P}$  NMR spectra. As a reversed-phase cartridge column, Sep-Pak Plus C18 cartridge (Waters) was used. Reversed phase HPLC analyses and purifications were performed using JASSO UV-4070 detector, PU2086 pump, CO4060 column heater and LCNETII/ADC interface system and Waters XBridge C18 5  $\mu\text{m}$  10  $\times$  250 mm column. MALDI-TOF-MS was performed using ultrafleXtreme (Bruker Daltonics). The absorption coefficients of ODNs were calculated according to the nearest-neighbor method using the Oligo Analyzer 3.1 (<http://sg.idtdna.com/calc/analyzer>) by assuming that the molar extinction coefficients of modified ODNs were identical to that of unmodified ODN.

## Synthesis of compound 2



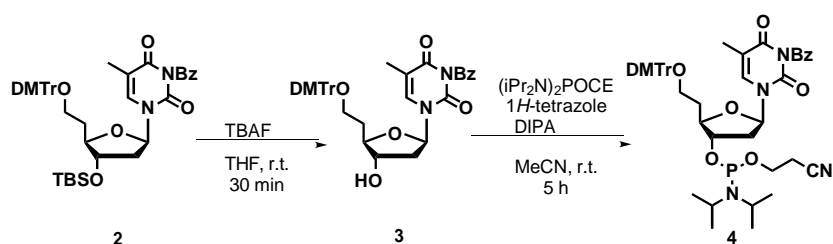
Compound 1 (1.90 g, 2.82 mmol) was dissolved in anhydrous pyridine (11.3 mL). To the solution, benzoyl chloride (655  $\mu\text{L}$ , 5.64 mmol), and *N,N*-diisopropylethylamine (1.95 mL, 11.3 mmol) were added. The resulting mixture was stirred at room temperature for 15 min. After reaction, methanol (6 mL) was added. The reaction mixture was diluted by ethyl acetate, and washed with sat.  $\text{NaHCO}_3$  twice, and sat.  $\text{NaCl}$ . The organic phase was dried over  $\text{Na}_2\text{SO}_4$ , filtered, and concentrated under reduced pressure.

The residue was purified by silica gel chromatography (N60) with hexane-ethyl acetate containing 1% triethylamine (9:1, v/v to 4:1, v/v) to afford compound **2** (1.91 g, 87%).

$^1\text{H}$  NMR (400 MHz,  $\text{DMSO-}d_6$ )  $\delta$  8.00 – 7.91 (m, 2H), 7.84 – 7.73 (m, 1H), 7.63 (d,  $J = 1.2$  Hz, 1H), 7.61 – 7.55 (m, 2H), 7.41 – 7.18 (m, 9H), 6.91 – 6.84 (m, 4H), 6.08 (t,  $J = 6.7$  Hz, 1H), 4.25 (ddd,  $J = 6.7, 3.8, 3.8$  Hz, 1H), 3.84 (td,  $J = 6.8, 3.8$  Hz, 1H), 3.72 (s, 3H), 3.72 (s, 3H), 3.08 (t,  $J = 6.8$  Hz, 2H), 2.37 (ddd,  $J = 13.6, 6.7, 6.7$  Hz, 1H), 2.10 (ddd,  $J = 13.6, 6.7, 3.8$  Hz, 1H), 1.93 (q,  $J = 6.8$  Hz, 2H), 1.86 (d,  $J = 1.2$  Hz, 3H), 0.85 (s, 9H), 0.04 (s, 3H), 0.03 (s, 3H).  $^{13}\text{C}$  NMR (101 MHz,  $\text{DMSO-}D_6$ )  $\delta$  169.6, 162.5, 158.1, 149.0, 145.2, 137.1, 135.9, 135.8, 135.6, 131.1, 130.4, 129.6, 129.5, 127.8, 127.6, 126.7, 113.2, 109.8, 85.5, 84.2, 83.6, 74.7, 60.2, 55.0, 33.4, 25.7, 17.6, 12.1, -4.7, -4.9.

MS (ESI) calcd. for  $\text{C}_{45}\text{H}_{52}\text{N}_2\text{NaO}_8\text{Si}^+$   $[\text{M}+\text{Na}]^+$  799.3385, found 799.3365

## Synthesis of compound 4



Compound **2** (1.90 g, 2.45 mmol) was dissolved in THF (9 mL). To the solution, 1 mol/L tetrabutylammonium fluoride in THF (3.67 mL) was added. The resulting mixture was stirred at room temperature for 30 min. The reaction mixture was diluted by ethyl acetate, and washed with  $\text{H}_2\text{O}$  twice, and sat. NaCl. The organic phase was dried over  $\text{Na}_2\text{SO}_4$ , filtered, and concentrated under reduced pressure. The residue was purified by silica gel chromatography (N60) with hexane-ethyl acetate containing 1% triethylamine (3:1, v/v to 1:1, v/v) to afford compound **3**. Compound **3** was rendered anhydrous by co-evaporation with dry pyridine five times, and with dry toluene five times then the residue was dissolved in anhydrous acetonitrile (22 mL). To the solution, diisopropylamine (216  $\mu\text{L}$ , 1.54 mmol), 1*H*-tetrazole (110 mg, 1.54 mmol) and 2-cyanoethyl *N,N,N',N'*-tetraisopropylphosphordiamidite (960  $\mu\text{L}$ , 3.09 mmol) were added. The resulting mixture was stirred at room temperature for 5 h. The reaction mixture was diluted by ethyl acetate, and washed with sat.  $\text{NaHCO}_3$  three times, and sat. NaCl. The organic phase was dried over  $\text{Na}_2\text{SO}_4$ , filtered, and concentrated under reduced pressure. The residue was purified by silica gel chromatography (Biotage® Sfar Silica HC D, 25 g) with hexane-ethyl acetate containing (2:1, v/v to 1:1, v/v) to afford compound **4** (1.56 g, 74%).

$^1\text{H}$  NMR (400 MHz,  $\text{CDCl}_3$ )  $\delta$  7.97 – 7.84 (m, 2H), 7.68 – 7.60 (m, 1H), 7.55 – 7.39 (m, 4H), 7.37 – 7.13 (m, 8H), 6.88 – 6.75 (m, 4H), 6.26 – 6.12 (m, 1H), 4.41 – 4.29 (m, 1H), 4.23 – 4.10 (m, 1H), 3.86 – 3.64 (m, 8H), 3.64 – 3.49 (m, 2H), 3.34 – 3.21 (m, 2H), 2.64 – 2.43 (m, 3H), 2.19 – 1.99 (m, 2H), 1.96 – 1.81 (m, 4H), 1.22 – 1.11 (m, 12H).  $^{13}\text{C}$  NMR (101 MHz,  $\text{CDCl}_3$ )  $\delta$  169.1, 162.9, 158.6, 158.6, 149.4, 149.3, 145.2, 136.4, 136.3, 136.3, 135.2, 135.2, 135.1, 135.0, 131.7, 131.7, 130.7, 130.2, 130.2, 130.1, 130.1, 129.3, 128.3, 128.3, 128.2, 128.0, 127.9, 127.0, 126.9, 117.9, 117.8, 113.2, 113.2, 111.3, 111.2, 86.4, 86.3, 85.2, 85.0, 83.7, 83.6, 83.3, 83.2, 76.5, 76.1, 76.0, 60.3, 60.3, 58.3, 58.1, 58.1, 57.9, 55.4, 55.4, 43.5, 43.4, 39.3, 39.3, 39.3, 39.2, 39.2, 34.3, 34.3, 24.8, 24.8, 24.7, 24.7, 24.7, 24.7, 24.6, 20.6, 20.5, 20.5, 20.4, 12.9.  $^{31}\text{P}$  NMR (162 MHz,  $\text{CDCl}_3$ )  $\delta$  149.5, 149.1.

MS(ESI) calcd. for  $\text{C}_{48}\text{H}_{55}\text{N}_4\text{NaO}_9\text{P}^+$   $[\text{M}+\text{Na}]^+$  885.3599, found 885.3595.

## Preparation of oligonucleotides

ODNs were synthesized in 1  $\mu\text{mol}$  scale on solid-supports of controlled pore glass (CPG) with DNA synthesizer nS8-II (GeneDesign, Inc.) using standard phosphoramidite method. The natural DNA phosphoramidites (dT, dG(iBu), dA(Bz)) and the solid support (Glen Unysupport 1000) were purchased from Glen Research. The 5-methyl deoxycytosine phosphoramidite ( $\text{dm}^5\text{C}(\text{Bz})$ ) was purchased from Link Technologies Ltd. LNA phosphoramidites (LT, LA(Bz),  $\text{Lm}^5\text{C}(\text{Bz})$ , and LG(dmf)) were purchased from Hongene Biotech Corporation. All phosphoramidites except for  $\text{Lm}^5\text{C}(\text{Bz})$  were dissolved in anhydrous acetonitrile to prepare 0.1 M solution. The  $\text{Lm}^5\text{C}(\text{Bz})$  phosphoramidite was dissolved in anhydrous dichloromethane and anhydrous acetonitrile (1:1, v/v). The 0.25 M 5-Benzylthio-1*H*-tetrazole (BTT) in acetonitrile (Glen Research) was used as an activator. The coupling time for LNA phosphoramidites and modified residues was 12 min twice which was longer than that for the natural bases. The sulfurization was performed using 0.05 M Sulfurizing Reagent II (DDTT, Glen Research, Sterling, VA, USA) for 5 min twice after each coupling step. After synthesis of oligonucleotides, additional sulfurization was performed for 5 min four times. DMTr-on CPG solid support was treated with 40% triethylamine in acetonitrile for 30 min to remove the cyanoethyl protecting group from the phosphate groups. Cleavage from the CPG solid support was performed using 28% ammonium hydroxide for 1 h at room temperature and removal of the base-protecting group was then carried out for 16-21 h at 55°C. After removal of ammonium hydroxide by miVac Duo centrifuge evaporator (Genevac, Ipswich, UK), the crude mixture of ODNs were purified on Sep-Pak Plus C18 cartridge (Waters, Milford, MA, USA). ODNs were further purified by reversed phase HPLC using JASSO UV-4070 detector, PU2086 pump, CO4060 column

heater and LCNETII/ADC interface system and Waters XBridge C18 5  $\mu\text{m}$  10  $\times$  250 mm column. In this reversed phase HPLC system, a linear gradient (5-45%, 1%/min) of solvent I (MeOH) in solvent II (8 mM triethylamine, 100 mM hexafluoroisopropanol buffer) was used at 65 °C at a flow rate of 3.0 mL/min for 40 min. Purified ODNs were analyzed by reversed phase HPLC. Reversed phase HPLC was performed using JASSO MD4015 (PDA), PU408i (pump), CO4060 (column) and LCNETII/ADC (interface bow) system and Waters XBridge C18 5  $\mu\text{m}$  4.6  $\times$  150 mm column. In this reversed phase HPLC system, a linear gradient (5-45%, 1%/min) of solvent I (MeOH) in solvent II (8 mM triethylamine, 100 mM hexafluoroisopropanol buffer) was used at 65 °C at a flow rate of 1.0 mL/min for 40 min. MALDI-TOF-MS was performed using ultrafleXtreme (Bruker Daltonics). The RNAs including FAM-labelled RNAs were purchased from Eurofin or IDT and used without further purification.

### **UV melting experiments**

ODNs were dissolved in deionized distilled water and their concentration was determined from UV absorbance at 260 nm. The absorption coefficients of ODNs were calculated according to the nearest-neighbor method using the Oligo Analyzer 3.1 (<http://sg.idtdna.com/calc/analyzer>) by assuming that modified ODNs were identical to T by replacing 5'-HMT or 3'-HMT. The oligonucleotides (400 pmol each) were dissolved in 200  $\mu\text{L}$  of folding buffer (10 mM phosphate buffer (pH 7.0) with 100 mM NaCl and 0.1 mM EDTA). The final concentration of the duplex was 2.0  $\mu\text{M}$ . The temperature of solution was increased by 0.5°C/min from 25°C to 95°C and then decreased back to 25°C. The absorption at 260 nm was recorded and used to draw UV-melting curves. The measurement was carried out three times independently. The UV-melting curve was smoothed by the Savitzky-Golay method. Melting temperatures were calculated as the temperature that gave the maximum of the first derivation of the UV-melting curves. The average of three  $T_m$  values was used to determine the final  $T_m$  value.

### **RNase H cleavage patterns**

5'-FAM labeled RNA (100 nM) was mixed to the ASO (200 nM) and annealed in annealing buffer containing 50 mM Tris-HCl, 75 mM KCl, 125 $\mu\text{M}$  EDTA at pH 8.3. Then the 20  $\mu\text{L}$  solution containing RNase H (0.05 U/ $\mu\text{L}$ , E.Coli, TaKaRaBio, Japan), 50 mM Tris-HCl, 75 mM KCl, 20

mM MgCl<sub>2</sub> and 5 mM DTT at pH 8.3 was added to each duplex solution (80 µL) and the reaction was incubated at 37°C for 5 min. The 10 µL reaction mixture was collected and stopped by adding 10 µL stop solution containing 10 M urea, 50 mM EDTA • 2Na and 0.1 wt% Bromophenol Blue. Samples separated on 20% denaturing polyacrylamide gel were detected using a Typhoon™ FLA 9500 and analyzed with ImageJ software (ver 1.53). RNA sequence used: 5' -GGUGAUGGCAAUUUA, and 5' -GGUGAUGACAAUUUA



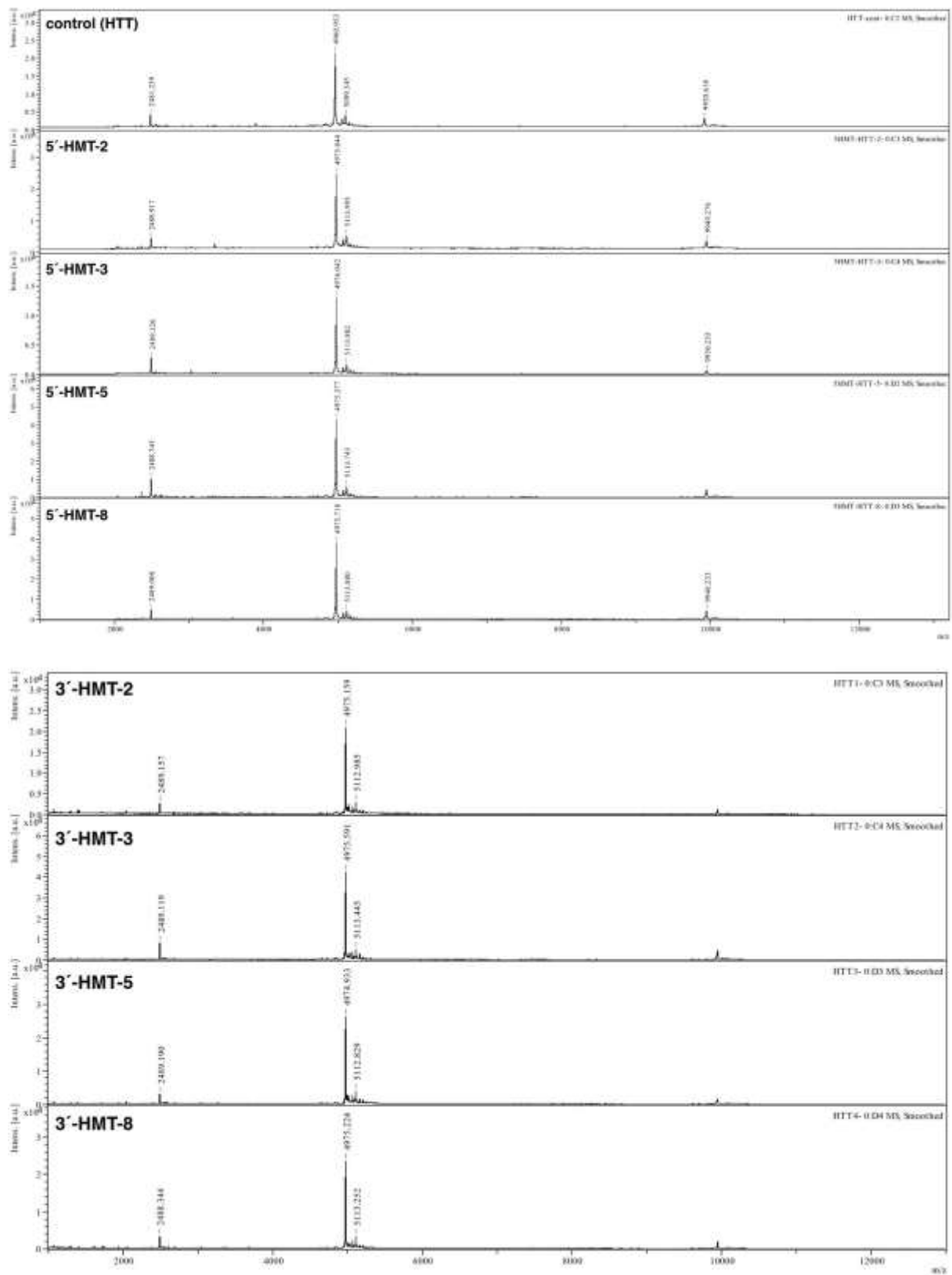
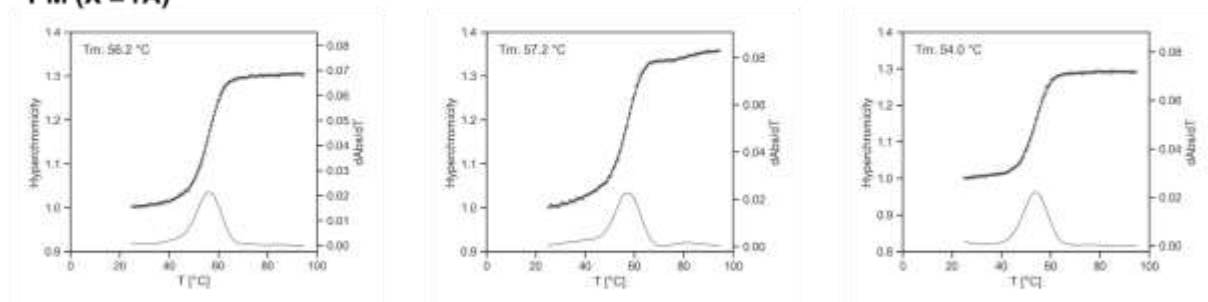


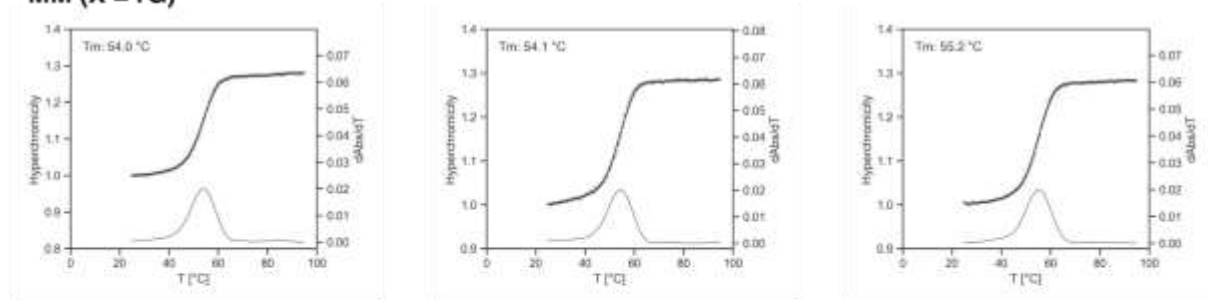
**Figure S1.** MALDI-TOF-MS chart of HTT-targeting antisense oligonucleotides.

control 5'- TAA attgtcatc ACC  
 RNA 3'-r(AUU UAACXGAAG UGG)

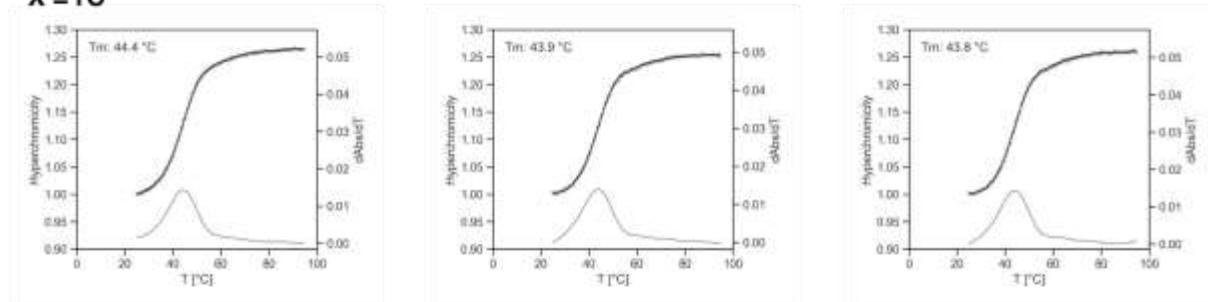
**PM (X = rA)**



**MM (X = rG)**



**X = rC**



**X = rU**

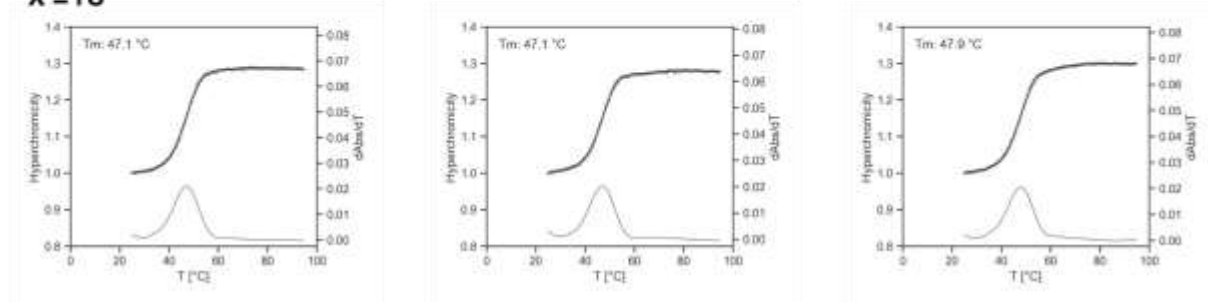
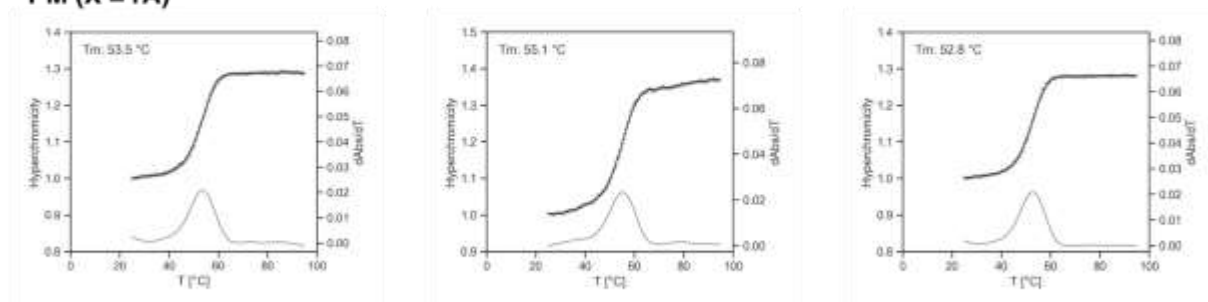


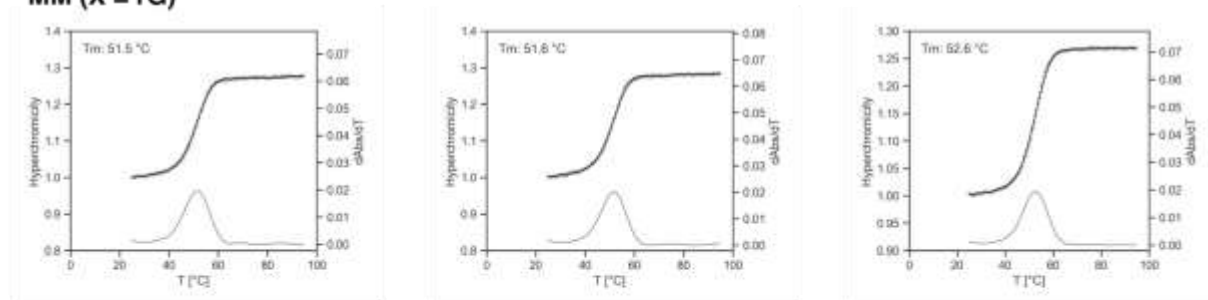
**Figure S2.** Melting curves of each oligonucleotide with RNAs.

5'-HMT-2    5'- TAA aYtgatcacc ACC    Y=5'-HMT  
 RNA        3'-r(AUU UAACXGAAG UGG)

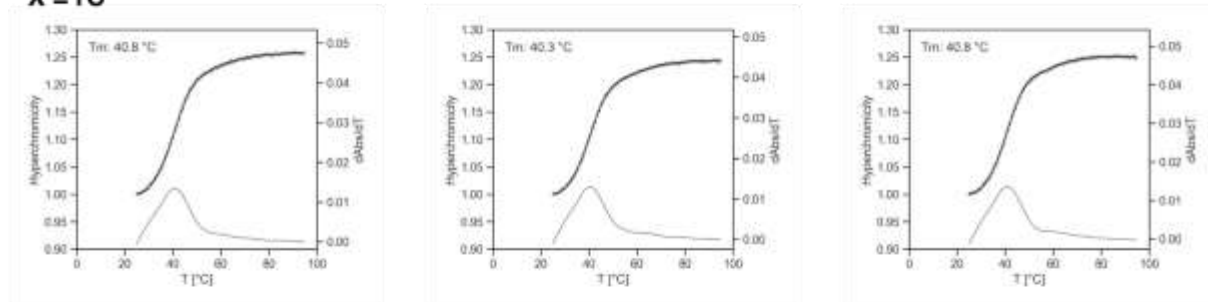
**PM (X = rA)**



**MM (X = rG)**



**X = rC**



**X = rU**

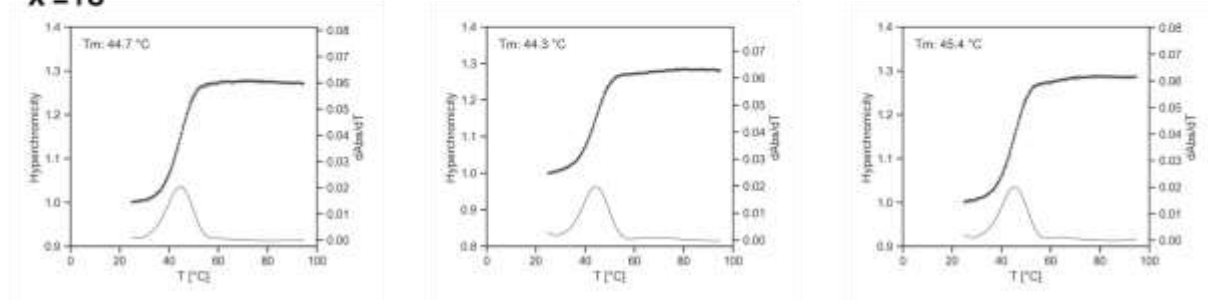
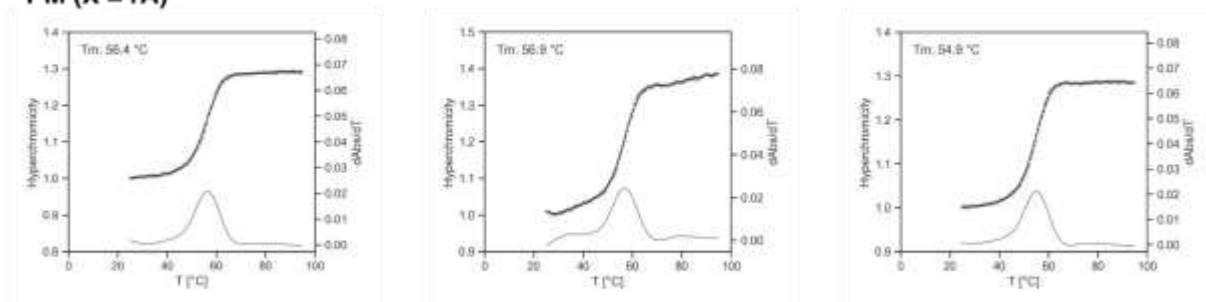


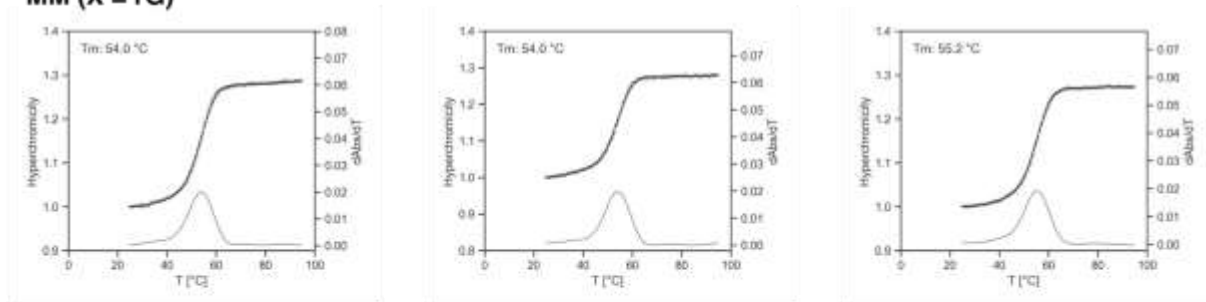
Figure S2. continued.

5'-HMT-3    5'- TAA atYgtcatc ACC    Y=5'-HMT  
 RNA        3'-r(AUU UAACXGAAG UGG)

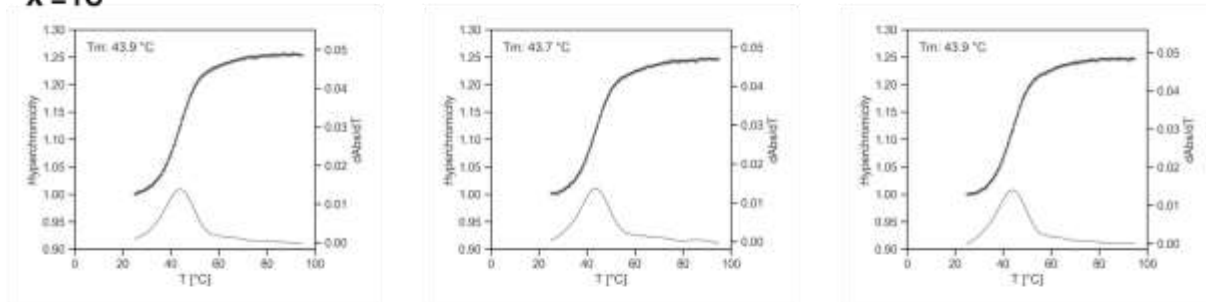
**PM (X = rA)**



**MM (X = rG)**



**X = rC**



**X = rU**

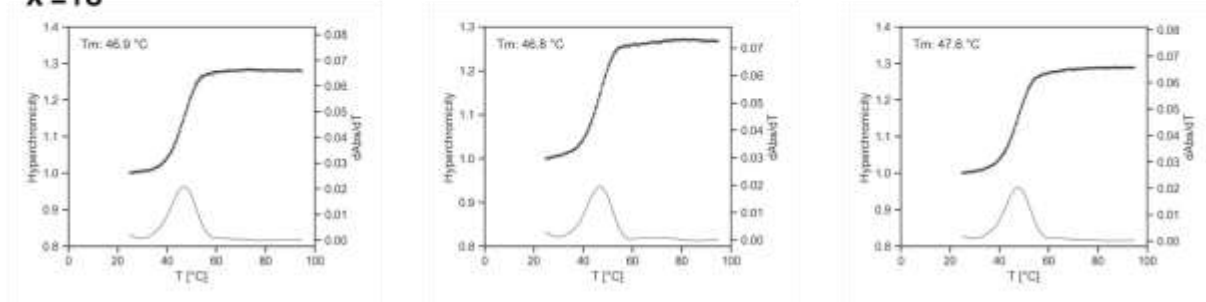
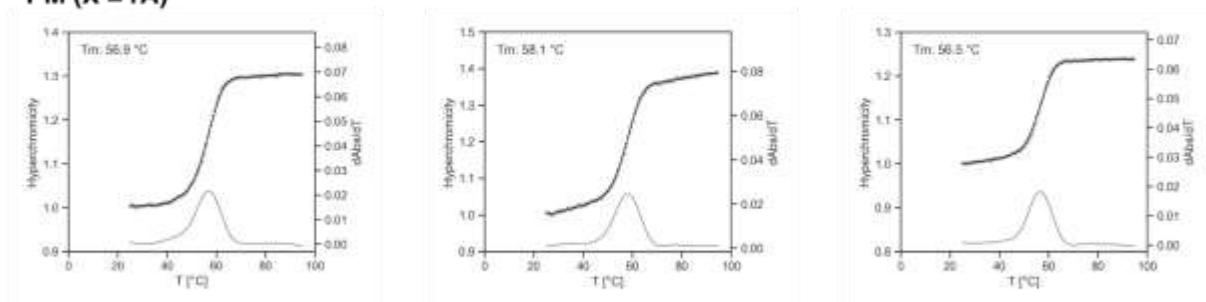


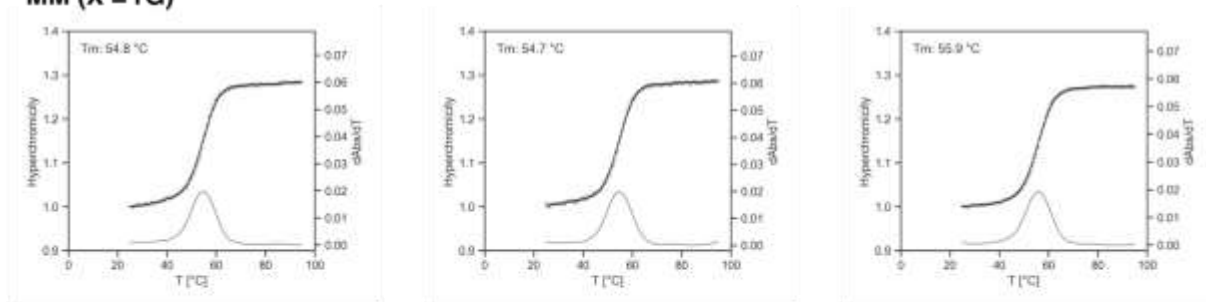
Figure S2. continued.

5'-HMT-5    5'- TAA attgYcatc ACC    Y = 5'-HMT  
 RNA        3'-r(AUU UAACXGAAG UGG)

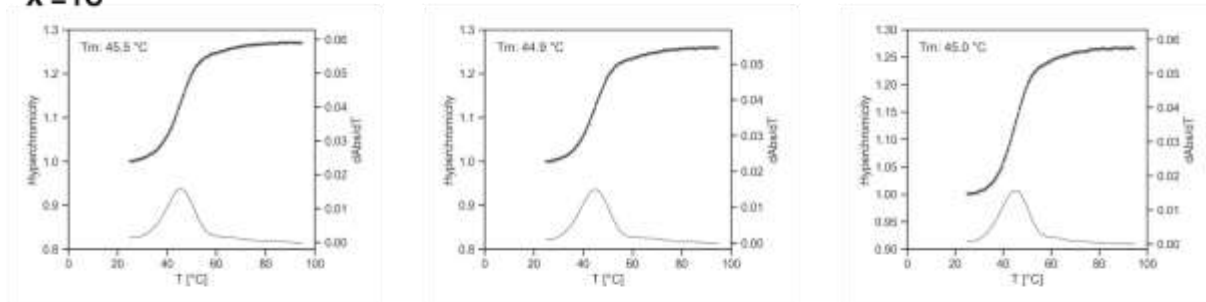
**PM (X = rA)**



**MM (X = rG)**



**X = rC**



**X = rU**

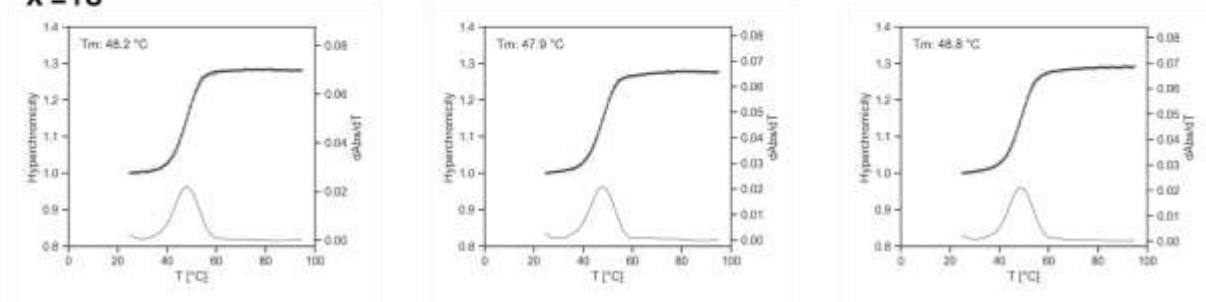
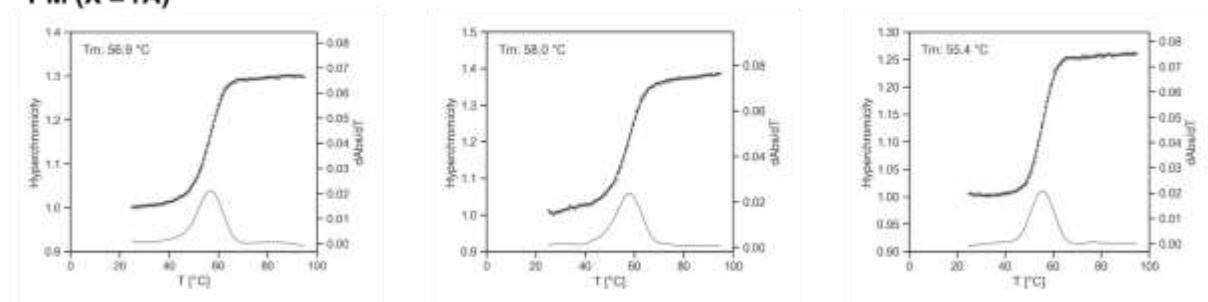


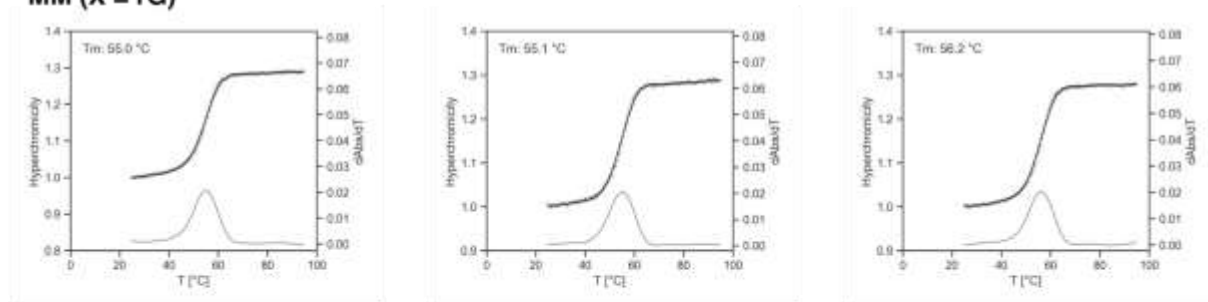
Figure S2. continued.

5'-HMT-8    5'- TAA attgtcaYc ACC    Y = 5'-HMT  
 RNA        3'-r(AUU UAACXGAAG UGG)

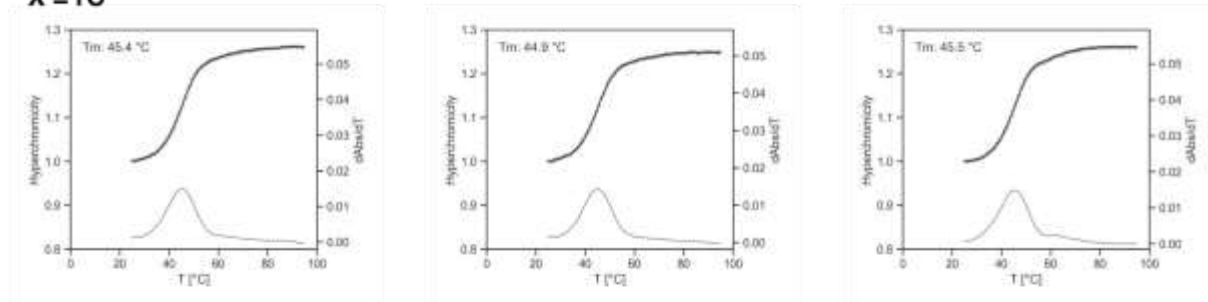
**PM (X = rA)**



**MM (X = rG)**



**X = rC**



**X = rU**

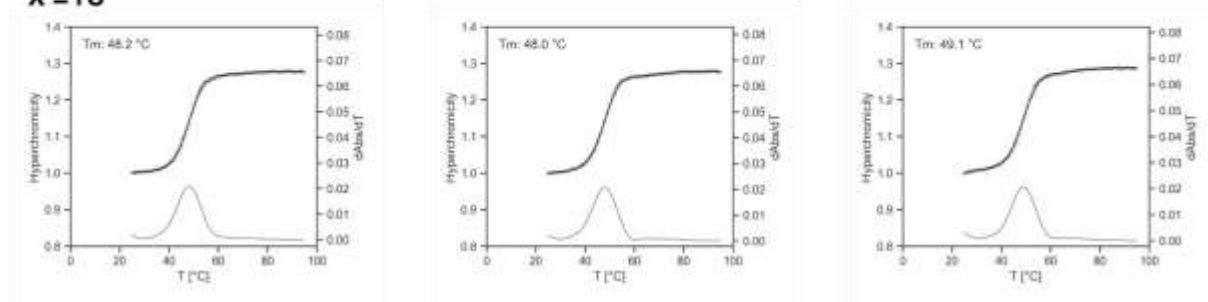
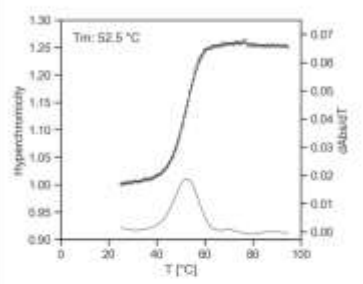
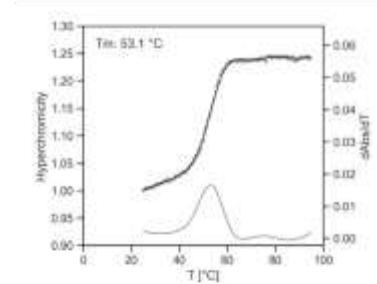
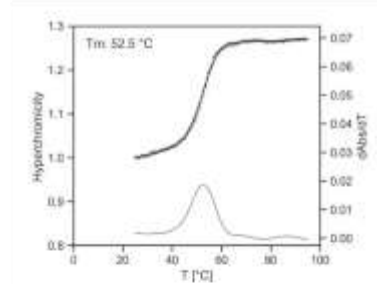
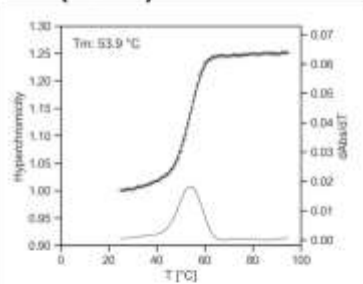


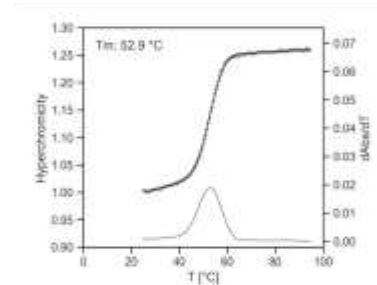
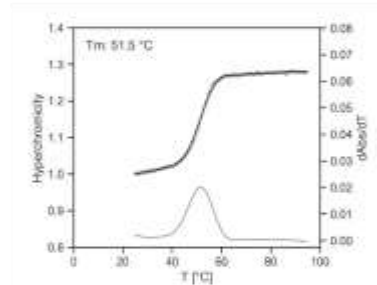
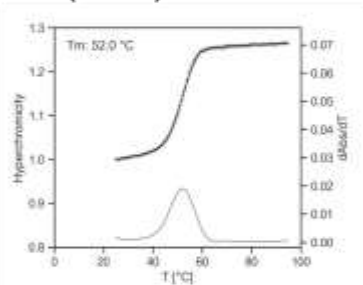
Figure S2. continued.

3'-HMT-2 5'- TAA aYgtcatc ACC Y=3'-HMT  
 RNA 3'-r(AUU UAACXGAAG UGG)

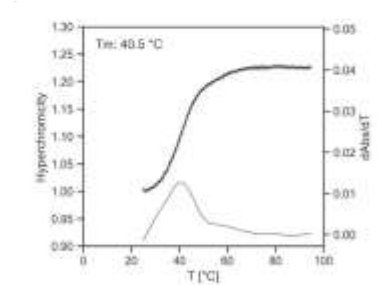
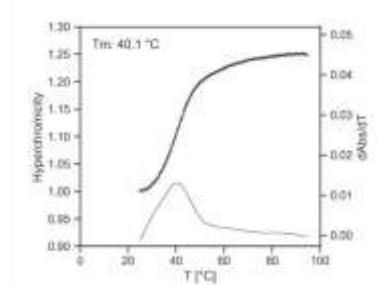
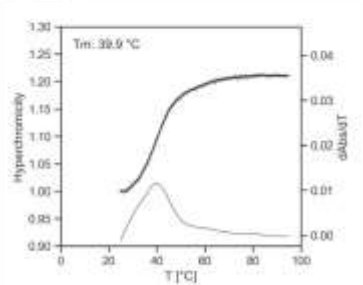
**PM (X = rA)**



**MM (X = rG)**



**X = rC**



**X = rU**

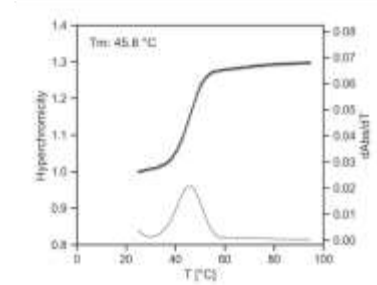
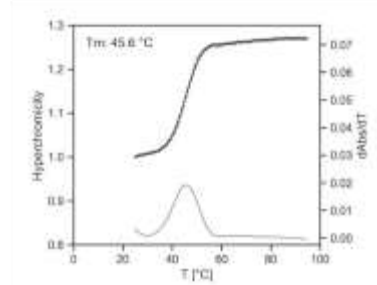
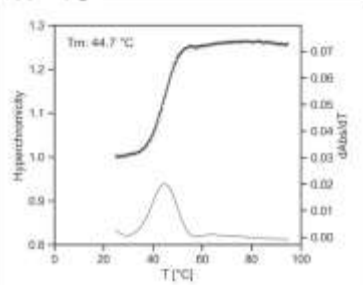
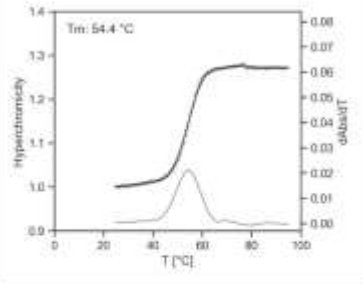
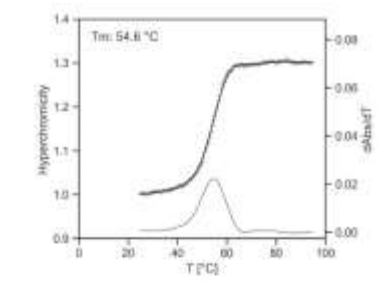
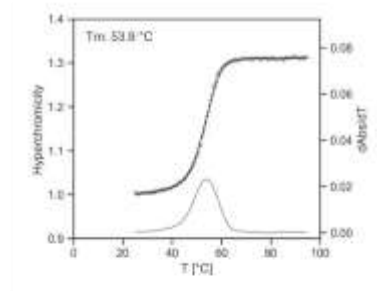
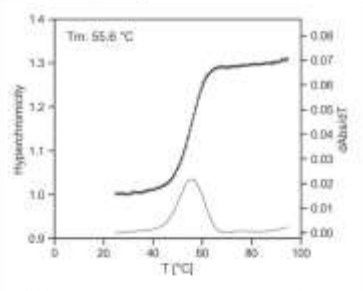


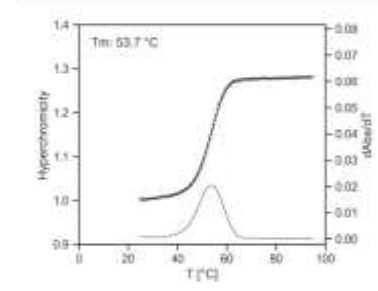
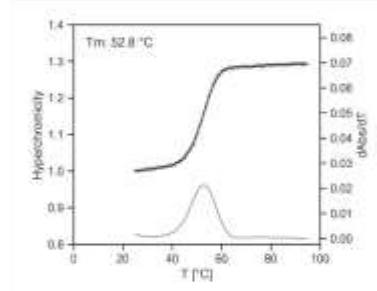
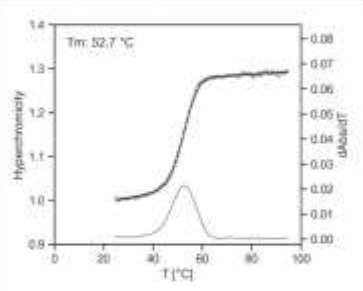
Figure S2. continued.

3'-HMT-3 5'- TAA atYgtcatc ACC Y=3'-HMT  
 RNA 3'-r(AUU UAACXGAAG UGG)

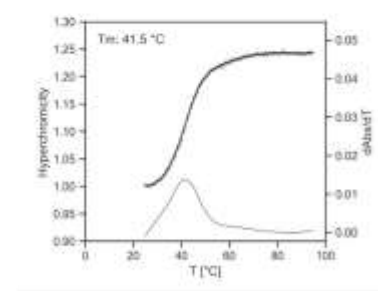
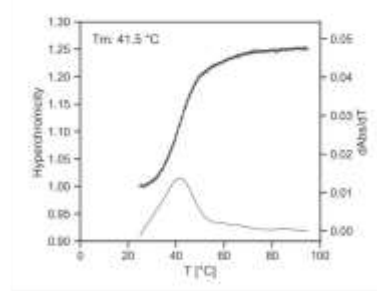
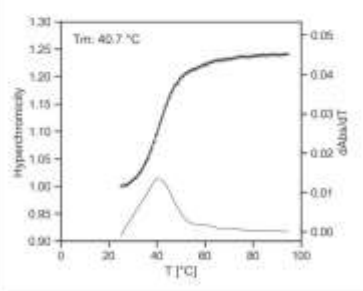
**PM (X = rA)**



**MM (X = rG)**



**X = rC**



**X = rU**

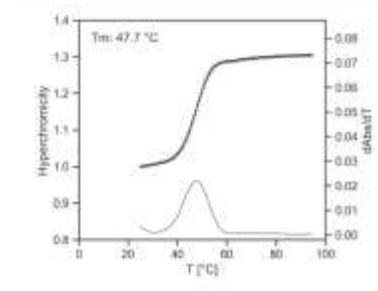
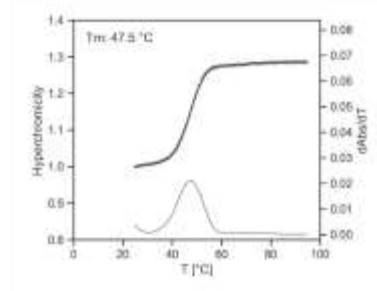
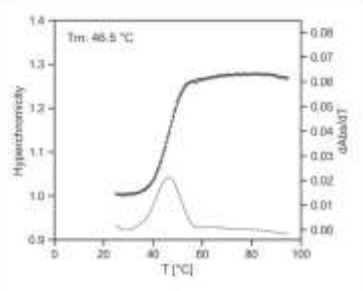
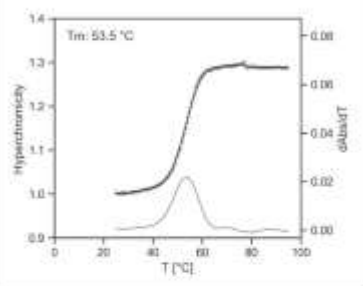
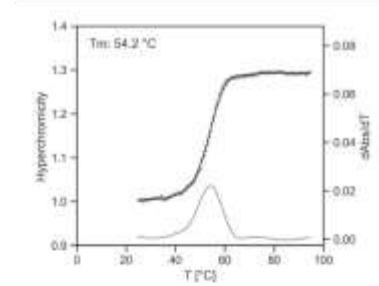
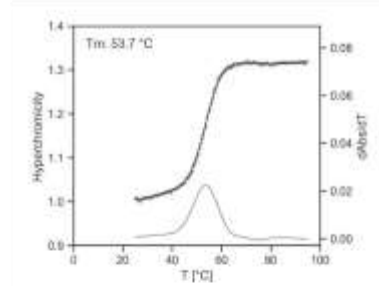
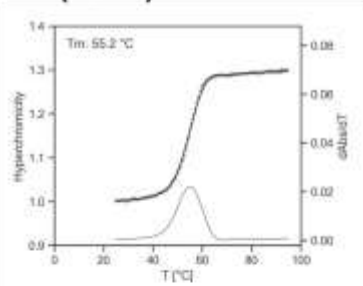


Figure S2. continued.

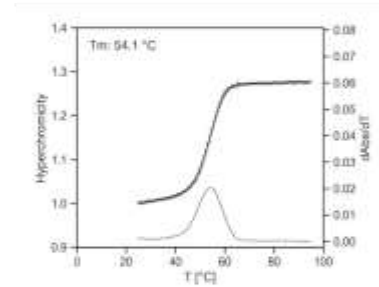
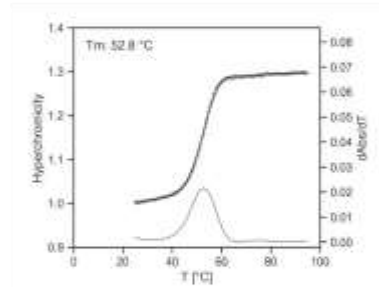
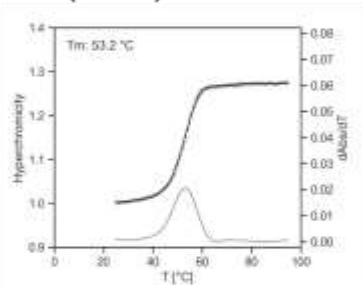


3'-HMT-5    5'- TAA attgYcatc ACC    Y = 3'-HMT  
 RNA        3'-r(AUU UAACXGAAG UGG)

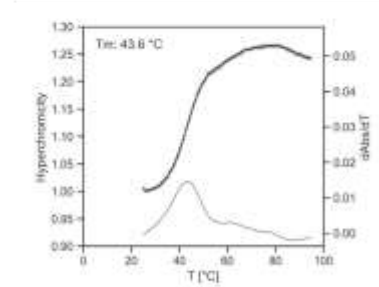
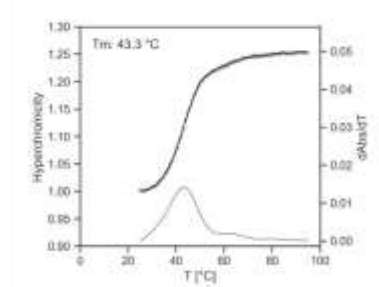
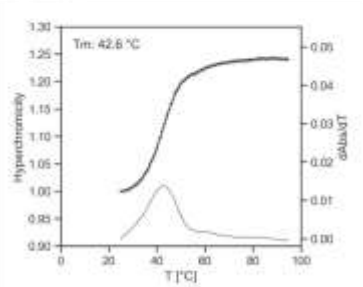
**PM (X = rA)**



**MM (X = rG)**



**X = rC**



**X = rU**

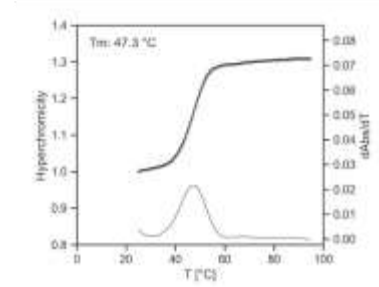
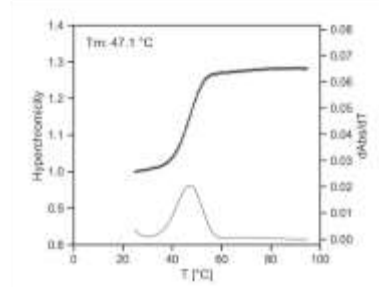
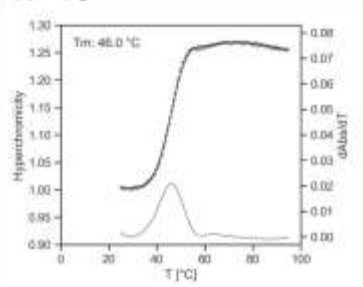
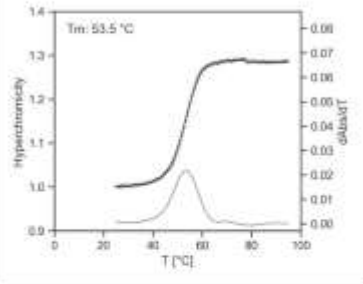
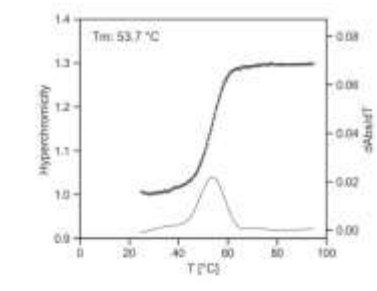
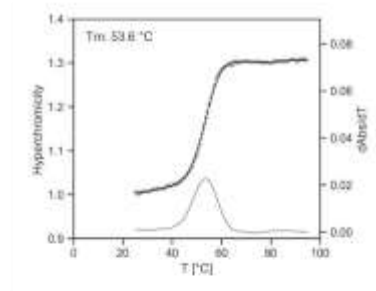
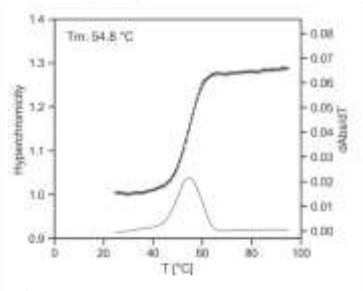


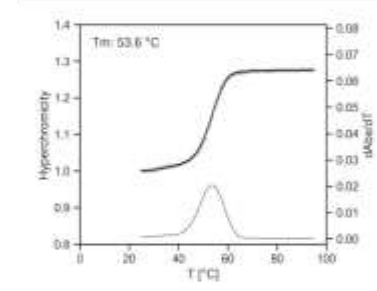
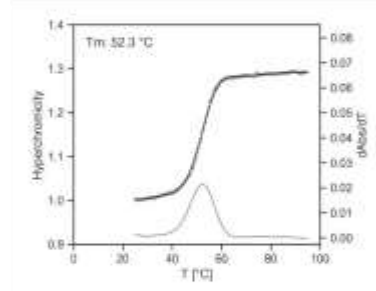
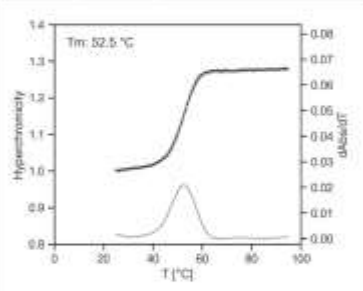
Figure S2. continued.

3'-HMT-8    5'- TAA attgtcaYc ACC    Y = 3'-HMT  
 RNA        3'-r(AUU UAACXGAAG UGG)

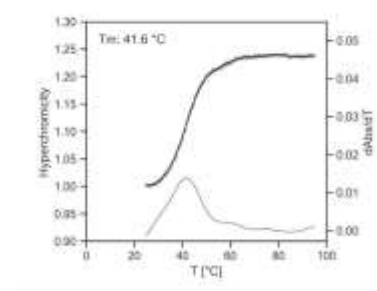
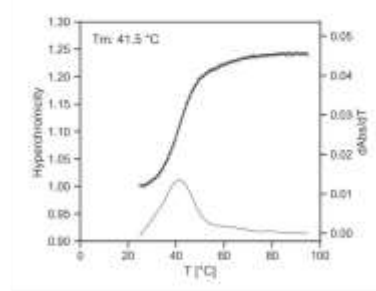
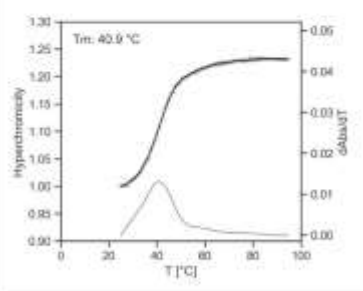
**PM (X = rA)**



**MM (X = rG)**



**X = rC**



**X = rU**

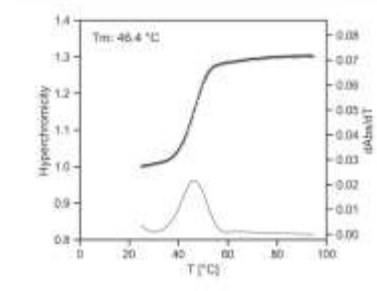
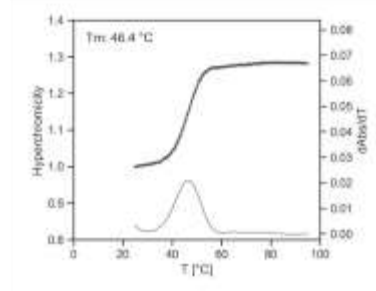
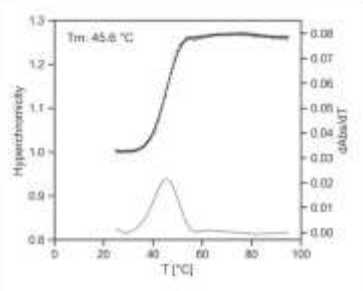
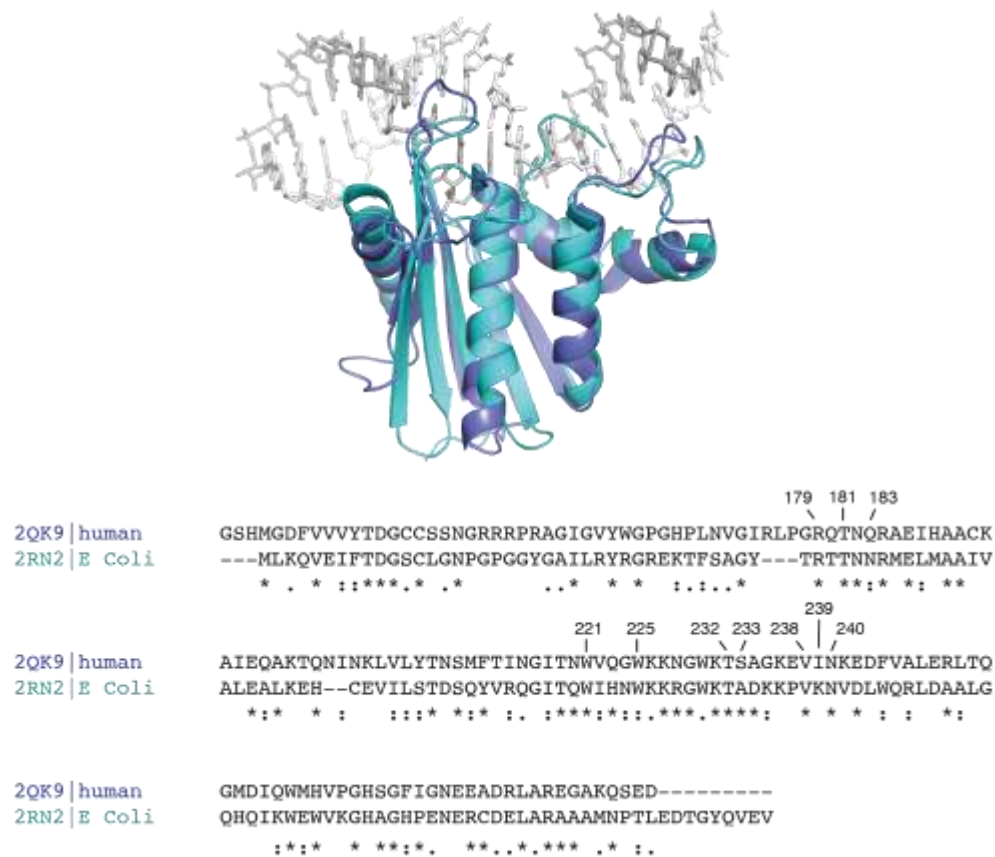
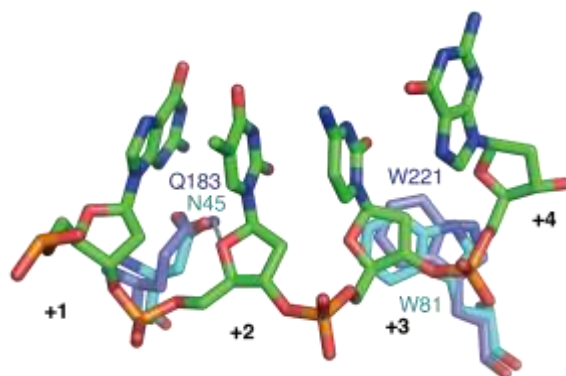


Figure S2. continued.

A)



B)



**Figure S3.** E. Coli RNase H (2RN2) and human RNase H1 catalytic domain (2QK9).

A) Superimposed structures of E. Coli RNase H (2RN2) and human RNase H1 catalytic domain (2QK9).

B) Recognition of deoxyribose ring at +2 and +3 positions. Although the X-ray structure of E. Coli RNase H does not contain DNA/RNA duplex, it was well superimposed to the human RNase H catalytic domain - DNA/RNA complex (RMSD 1.680 Å (631 atoms), align command in pymol).

**Table S1.** Positional relative kinetic constants ( $k_{rel,i}$ ) of 5'-HMT modification.

	-3	-2	-1	0	+1	+2	+3	+4	+5	+6	+7
5' HMT-2	0.98	1.06	1.01	1.03	0.80						
5' HMT-2	1.00	1.03	0.97	0.89	0.92						
5' HMT-2	0.99	1.04	0.96	1.00	0.79						
5' HMT-3		0.97	0.64	0.86	0.36	0.64					
5' HMT-3		0.87	0.92	0.88	0.48	0.72					
5' HMT-3		0.86	0.85	0.82	0.61	0.59					
5' HMT-5				1.05	0.23	0.47	0.34	0.41			
5' HMT-5				0.61	0.65	0.50	0.38	0.51			
5' HMT-5				0.75	0.67	0.50	0.32	0.41			
5' HMT-8							0.15	0.34	1.87	2.05	1.64
5' HMT-8							0.11	0.27	1.73	1.84	1.70
5' HMT-8							0.09	0.23	1.73	1.73	1.63
average	0.99	0.97	0.89	0.88	0.61	0.57	0.23	0.36	1.78	1.87	1.66
std	0.01	0.09	0.13	0.14	0.22	0.10	0.13	0.10	0.08	0.17	0.04

**Table S2.** Positional relative kinetic constants ( $k_{rel,i}$ ) of 3'-HMT modification.

	-3	-2	-1	0	+1	+2	+3	+4	+5	+6	+7
3' HMT-2	1.08	0.76	0.80	1.20	0.34						
3' HMT-2	1.16	0.92	0.88	0.83	0.37						
3' HMT-2	1.13	0.95	0.79	1.22	0.40						
3' HMT-3		0.68	0.54	0.56	0.45	0.10					
3' HMT-3		0.71	0.71	0.70	0.33	0.08					
3' HMT-3		0.77	0.78	0.59	0.68	0.15					
3' HMT-5				0.85	0.31	0.01	0.54	1.36			
3' HMT-5				0.86	0.47	0.07	0.44	1.64			
3' HMT-5				0.70	0.69	0.08	0.55	1.44			
3' HMT-8							0.70	0.74	1.09	1.16	1.07
3' HMT-8							0.60	0.81	1.10	1.13	1.10
3' HMT-8							0.69	0.83	0.99	1.44	1.13
average	1.12	0.80	0.75	0.83	0.45	0.08	0.58	1.14	1.06	1.24	1.10
std	0.04	0.11	0.12	0.24	0.14	0.04	0.10	0.39	0.06	0.17	0.03

## Derivation of equations used in this study.

Under the assumption of first-order kinetics, the cleavage reaction is expressed by the following.

$$\frac{d[R]}{dt} = -k[R] \quad (1)$$

where  $[R]$  denotes the amount of intact RNA and  $k$  is the overall kinetic constant. By integration of above equation, the equation becomes

$$\frac{[R]}{[R]_0} = f_{234} = \exp(-kt) \quad (2)$$

where  $[R]_0$  is the initial concentration of RNA and  $f_{RNA}$  is the fraction of residual RNA. We defined the relative kinetic constant  $k_{rel}$  as the ratio of the overall kinetic constant of modified ASO  $k_m$  and that of **control**  $k_c$ .

$$k_{rel} = \frac{k_m}{k_c} = \frac{\ln(f_{234,c})}{\ln(f_{234,m})} \quad (3)$$

where  $f_{RNA,m}$  denotes the fraction of residual RNA in modified ASO and  $f_{RNA,c}$  denotes the fraction of residual RNA in **control**. This ratio can apply to any reaction interval if the reaction is followed by first-order kinetics.

Under approximation by parallel first-order kinetics, the cleavage product  $[C_i]$  and kinetic constant of  $i$ -th reaction  $k_i$  have the following relationship.

Here,

$$\frac{d[C_E]}{dt} = k_E[R] \quad (4)$$

$$[C] = G[C_E] \quad (5)$$

$$k = G k_E \quad (6)$$

By using equation (2), equation (4) will be:

$$\frac{d[C_E]}{dt} = k_E[R]_0 \exp(-kt) \quad (7)$$

Since the initial cleavage product  $[C]_0$  is none, the integrated form will be:

$$\frac{[C_E]}{[R]_0} = \frac{k_E}{k} (1 - \exp(-kt)) \quad (8)$$

Thus,

$$[R]_0 = \frac{[C]}{k} \frac{k}{k_E} \frac{1}{1 - \exp(-kt)}$$

$k$

$$\frac{[C_E]}{[C]} = \frac{k_E}{k = p_E} \quad (9)$$

where  $p_E$  is the fraction of  $i$ -th cleavage product  $[C_i]$  over the sum of cleavage products  $[C]$ . Above equation (9) can be used for **control** as well as modified ASO. We defined a positional relative  $i$ -th kinetic constant  $k_{rel,i}$  as the ratio of  $i$ -th kinetic constant by modified ASO  $k_{m,i}$  and the corresponding kinetic constant by **control**  $k_{c,i}$ .

Therefore,

$$k_{9;:,E} = \frac{k_{<_E}}{k} = \frac{p_{<_E} k_{<_E}}{p_{=E} k_{=E}} = \frac{p_{<_E}}{p_{=E}} k_{9;:,E} \quad (10)$$

$$p_{<_E} = \frac{k_{9;:,E}}{k_{9;:,E}} p_{=E} \quad (11)$$

If the effect of backbone modification is independent of the effect of mismatch base pair,  $k_{rel,i}$  can be used in a mismatched duplex. Thus,

$$p_{<_E(<<)} = \frac{k_{9;:,E}}{k_{9;:(<<)}} p_{=E(<<)} \quad (11)$$

where  $k_{rel(mm)}$  is the ratio of overall kinetic constant of modified ASO/**MM** and that of **control/MM**.

Since the sum of  $p_{<_E(<<)}$  is 1,  $k_{rel(mm)}$  can be removed as followed.

$$p_{<_E(<<)} = \frac{k_{9;:,E}}{\sum_E k_{9;:,E}^0} p_{=E(<<)} = \frac{k_{9;:,E}}{\sum_E k_{9;:,E}^0} \cdot p_{=E(<<)} \quad (13)$$

Thus,  $p_{<_E(<<)}$  can be calculated by using control experiment values ( $p_{=E(<<)}$ ) and  $k_{rel,i}$ . The

relationship between observed  $p_{<_E(<<)}$  and calculated  $p_{<_E(<<)}$  was shown in Figure 5B and Figure S2.

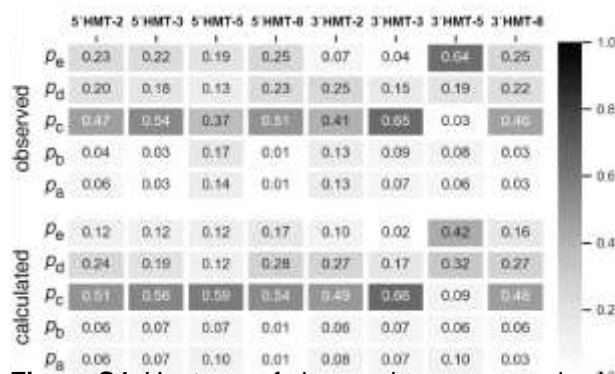
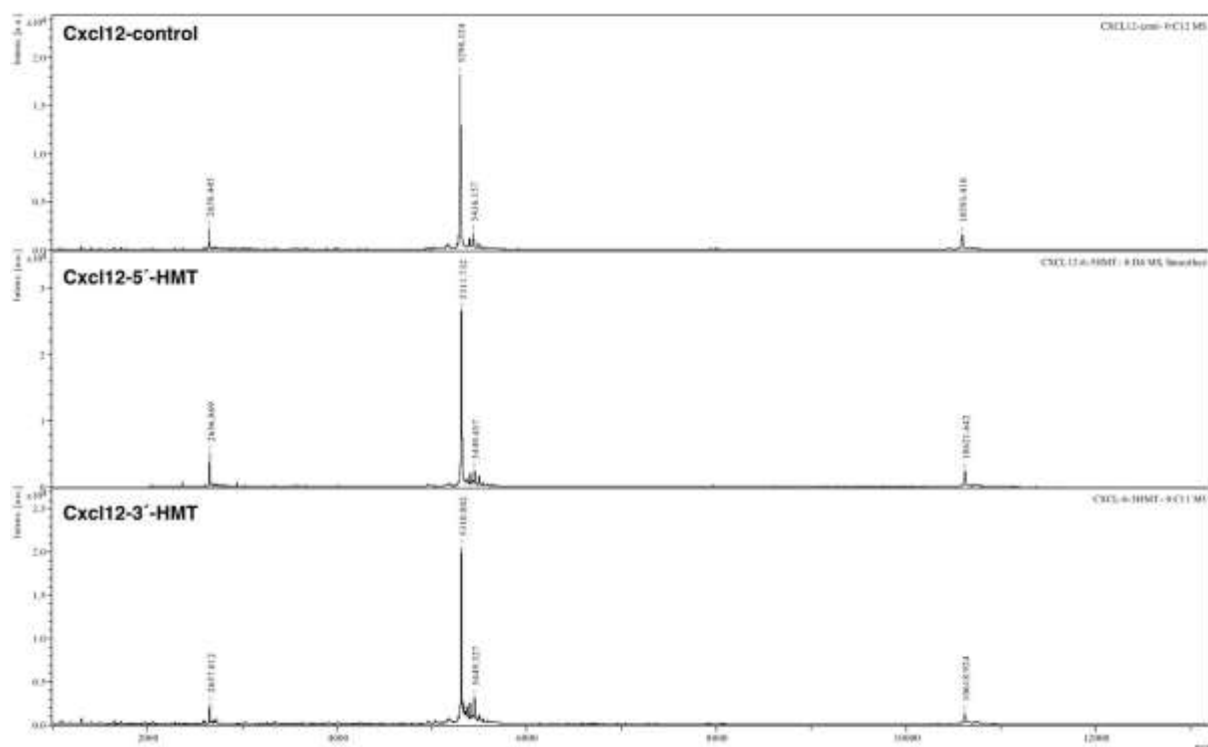


Figure S4. Heatmap of observed  $p_{m,i(mm)}$  and calculated  $p_{m,i(mm)}$



**Figure S5. MALDI-TOF-MS chart of Cxcl12-targeting antisense oligonucleotides.**

Calculated value for **Cxcl12-control** [M+H]<sup>+</sup>: 5297.2, found: 5298.3.

Calculated value for **Cxcl12-5'-HMT** [M+H]<sup>+</sup>: 5311.3, found: 5311.7.

Calculated value for **Cxcl12-3'-HMT** [M+H]<sup>+</sup>: 5311.3, found: 5310.8.

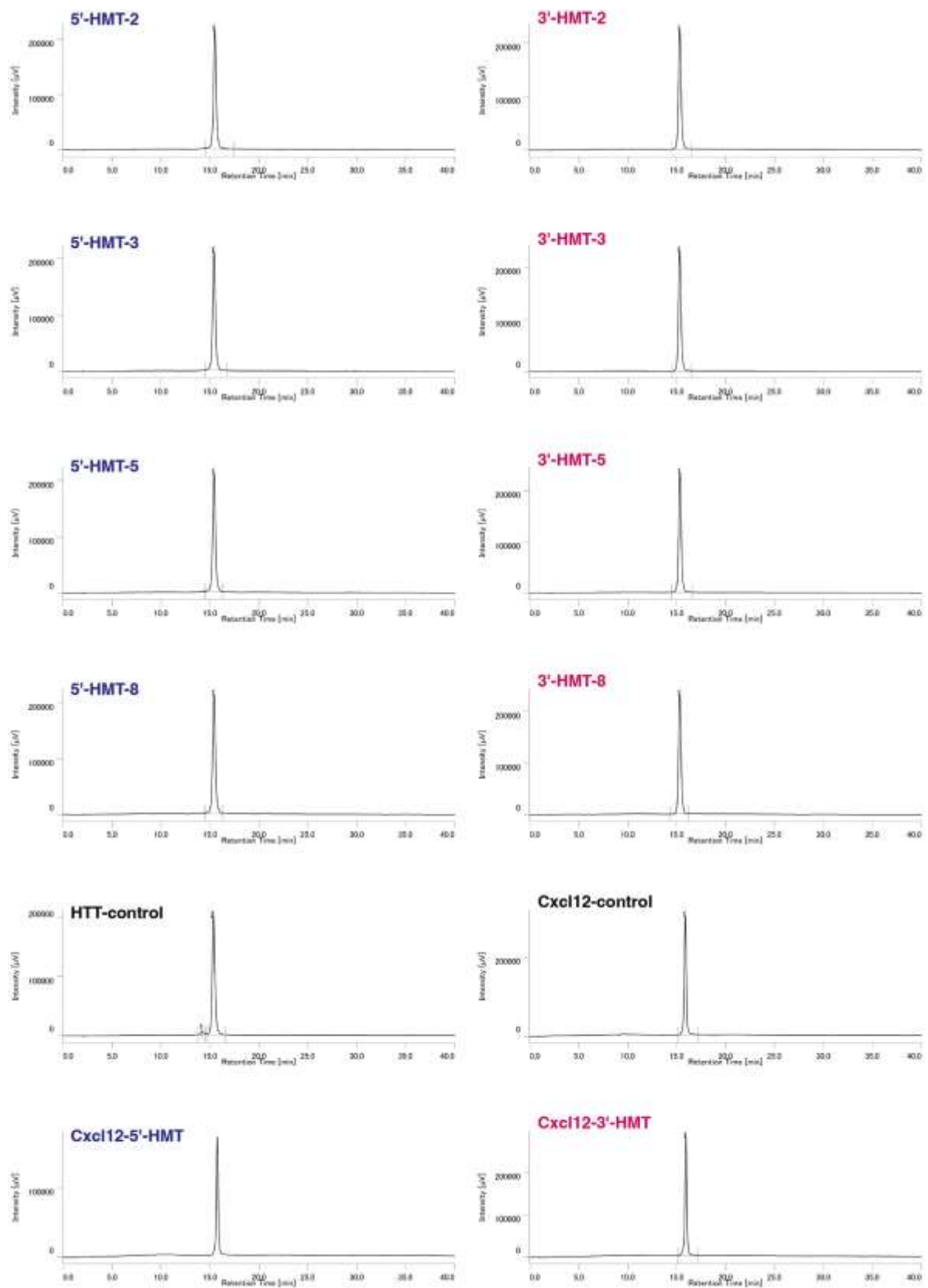
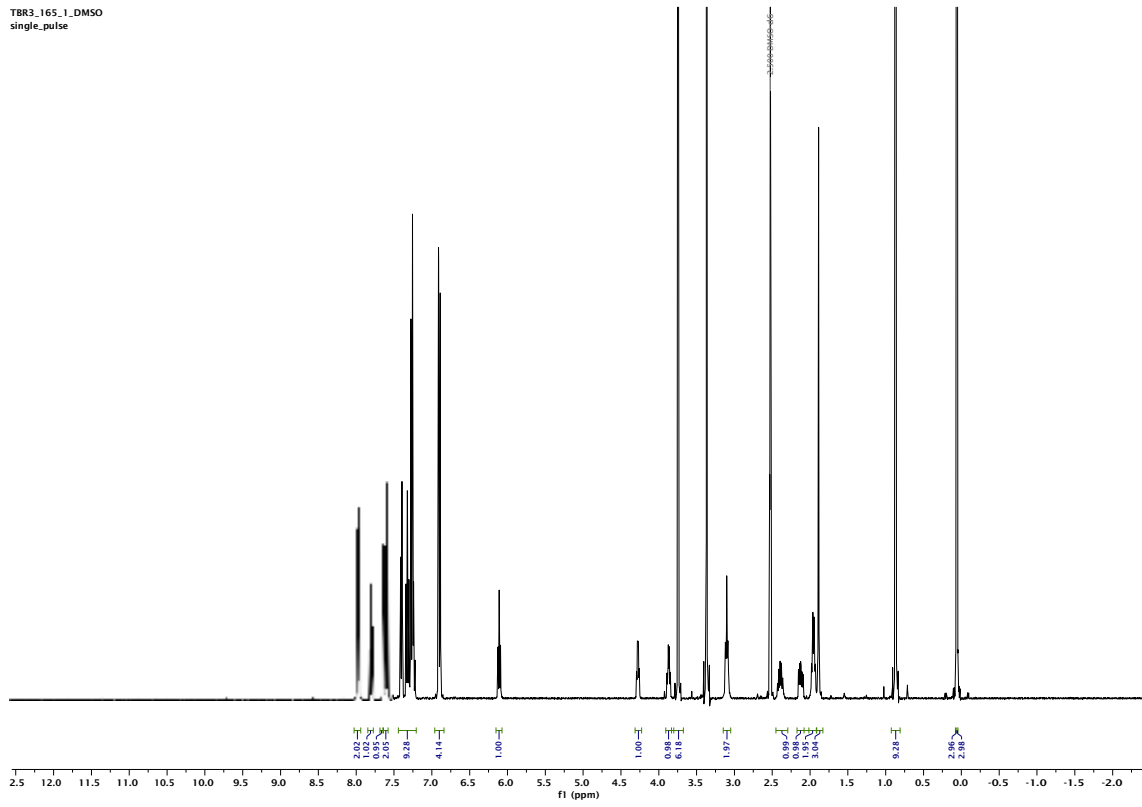


**Figure S6.** Reverse phase-HPLC chart of purified antisense oligonucleotides used in this study.



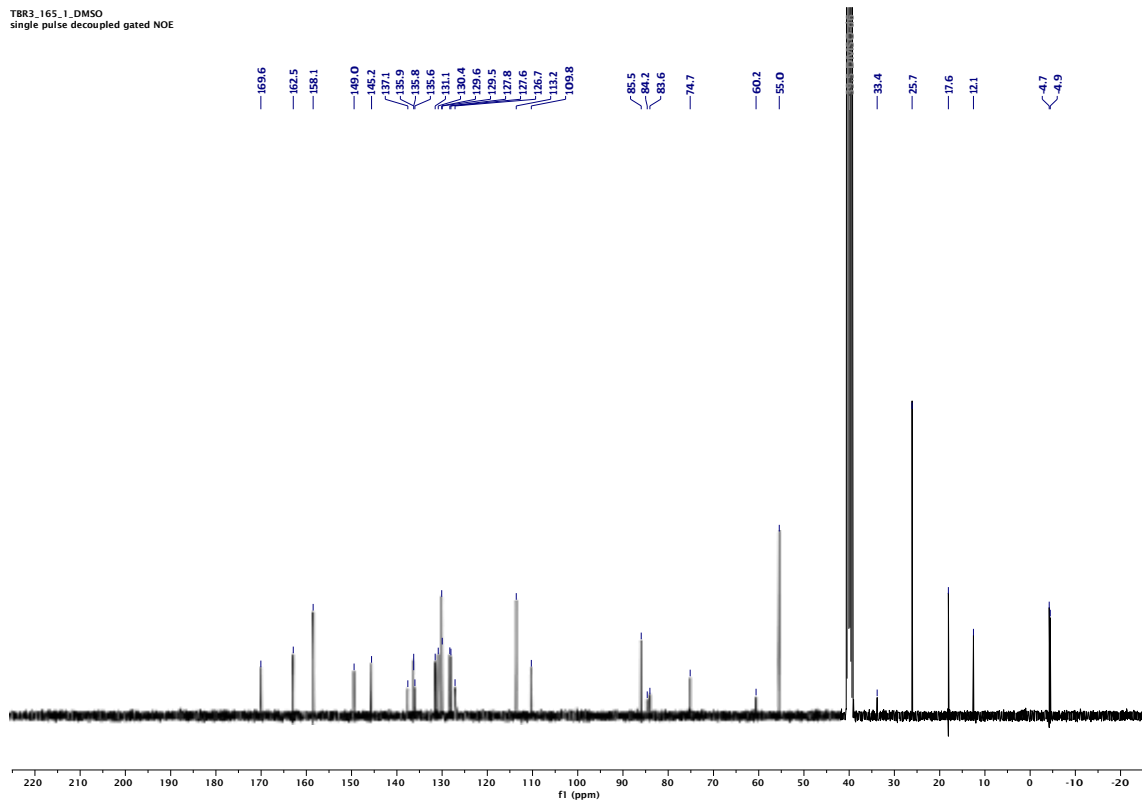
# <sup>1</sup>H-NMR of compound 2

TBR3\_165\_1\_DMSO  
single\_pulse

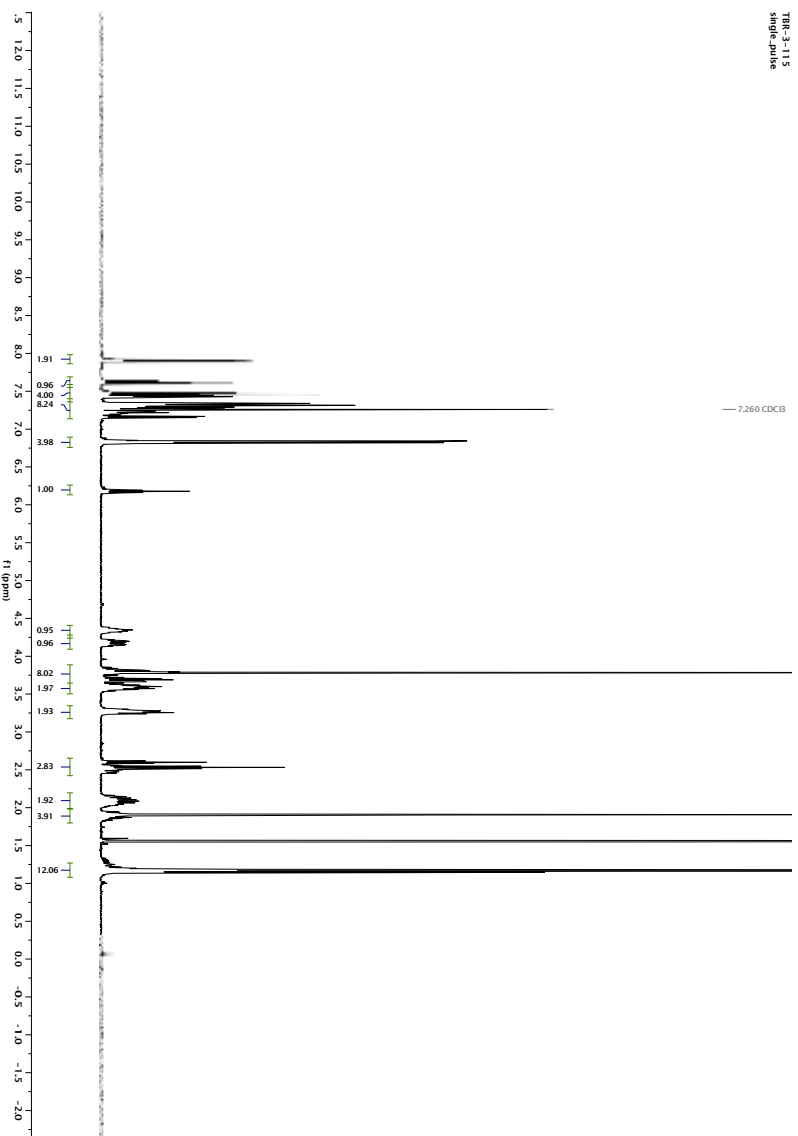


# <sup>13</sup>C-NMR chart of compound 2

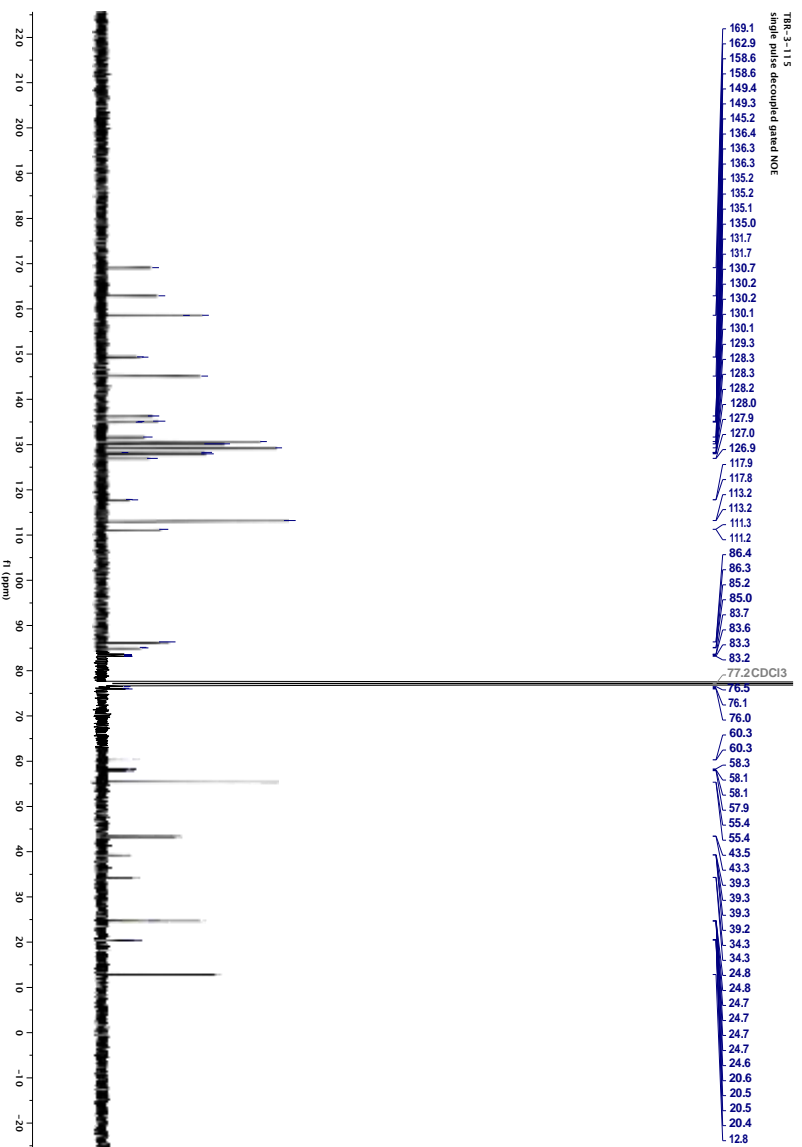
TBR3\_165\_1\_DMSO  
single pulse decoupled gated NOE



# <sup>1</sup>H-NMR of compound 4



# <sup>13</sup>C-NMR chart of compound 4



# 31P-NMR chart of compound 4

